Paper:

Configuration-Based Wheel Control for Step-Climbing Vehicle

Daisuke Chugo*, Kuniaki Kawabata, Hayato Kaetsu****
Hajime Asama***, and Taketoshi Mishima******

*The University of Electro-Communications, 5-1-5 Chofugaoka, Chofu, Tokyo 182-8585, Japan
E-mail: chugo@is.uec.ac.jp
**RIKEN (The Institute of Physical and Chemical Research), 2-1 Hirosawa, Wako, Saitama 351-0198, Japan
E-mail: {kuniakik, kaetsu}@riken.jp
***The University of Tokyo, 5-1-5 Kashiwanoha, Kashiwa, Chiba 277-8568, Japan
E-mail: asama@race.u-tokyo.ac.jp
****Saitama University, 255 Shimo-Ookubo, Saimata, Saitama 338-8570, Japan
E-mail: mishima@me.ics.saitama-u.ac.jp
[Received November 2, 2005; accepted November 20, 2006]

We propose a derivation of adaptable wheel rotation velocity for negotiating irregular terrain based on vehicle configuration. We developed a holonomic vehicle capable of negotiating steps and running around omnidirectionally on a flat floor using seven special wheels and two passive links. Each wheel has its actuator, requiring that the rotation velocity of individual wheels be coordinated, which is difficult due to changes rotation speed when the passive link negotiates the irregular terrain. Unstable rotation velocity calculated without considering the vehicle configuration causes wheel slippage and rotation error that adversely affect mobility on rough terrain. Because conventional general traction control cannot coordinate wheel velocity, we propose reference derivation that does so based on the vehicle configuration. In the sections that follow, we focus on (1) the derivation of individual wheel velocity during step climbing and (2) adaptation to wheel control reference while balancing rotation velocity among wheels. We confirm the feasibility of our proposal in experiments using our vehicle prototype.

Keywords: omnidirectional mobility, passive linkage, step climbing, wheel control

1. Introduction

Mobile robots operating in environments such as nuclear power plants, factories, welfare care facilities, and hospitals ideally must be able to negotiate narrow spaces and barriers such as vertical gaps, steps, and irregular terrain quickly to execute tasks efficiently. This requires omnidirectional mobility with no holonomic constraint on movement [1, 2] and step climbing ability.

Among the many omnidirectional mobile systems, e.g., legged, ball-shaped, and caterpillar, are devised thus far. Legged robots [3, 4] move in all directions and negotiate rough terrain, but many be complex and energy-inefficient, requiring actuators simply to maintain balance. Robots with ball-shaped wheels move in any direction [5], but many be unable to negotiate rough terrain. Special crawlers [6] proposed for omnidirectional mobile robots may move over irregular terrain but not over large steps. To meet these needs, we are developing holonomic omnidirectional stepclimbing vehicles [7].

Our prototype uses seven free-rolling wheels and passive links (**Fig. 1**). Its 12 cylindrical rollers [8] apply traction only in the direction of travel. Its wheels are actuated and generate omnidirectional movement through a suitable wheel arrangement and control.

Our vehicle's new passive links are more suitable than a general-purpose rocker-bogie suspension for step climbing [9, 10]. Free joint point 1 is the same height as the axle, so the vehicle negotiates the step smoothly when the wheel contacts it moving forward or backward [11]. No sensors or extra actuators are needed to negotiate barriers on the floor.

In using passive links and redundant actuators, our vehicle controller calculates control references for individual wheel based on a kinematic model [12], controlling actuators to use coordinates among wheels using PID-based control [13].

When a vehicle with passive links negotiates steps, individual wheel velocity differs because of changes in the vehicle configuration and its kinematic model, so wheel control references change in the vehicle configuration. Many mobile vehicles with passive links have been developed [14, 15], but most do not discuss the adjustment of control references using changes in vehicle configuration. Lamon et al., for examples, discuss vehicle configuration in three-dimensional odometry [15], but do not discuss the kinematics model on control reference of individual actuators.

Unsuitable control references calculated by a fixed kinematic model cause wheel slippage or rotation error, compromising vehicle movement [16] and, in the worst case, make the vehicle unstable (**Fig. 2**) when unstable

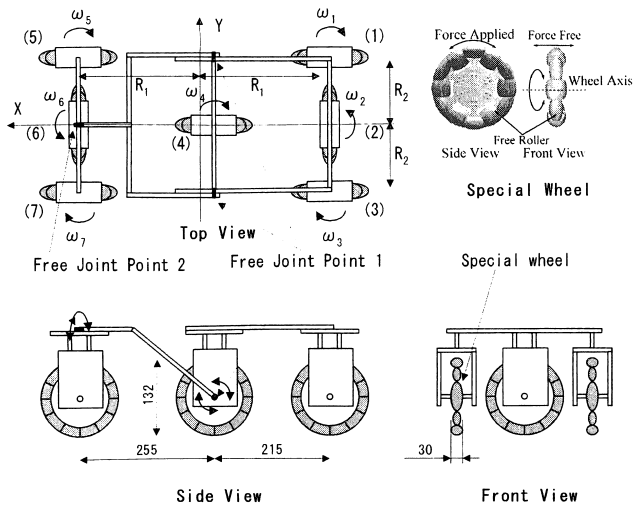

(a) Overview

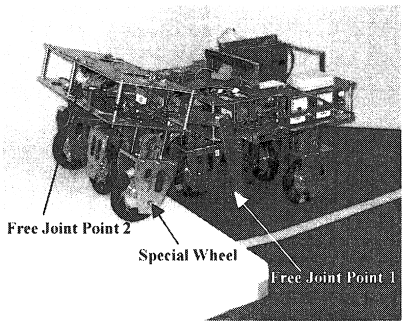

(b) Prototype

Fig. 1. Prototype.

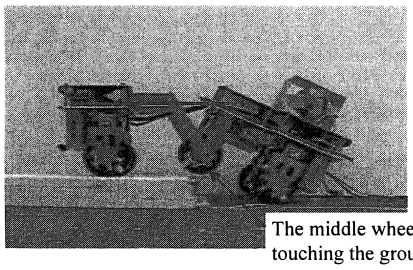

Fig. 2. Unstable positioning.

wheel control is used and unexpected force is applied to the free joints of the passive links, preventing the vehicle from negotiating. Such unstable control and unexpected force must be reduced to maximize traction.

Because mobile vehicles negotiating rough terrain generally control their wheel by using traction, we focused in previous works on wheel feedback control considering the output traction of individual wheels [17], but found it is difficult to coordinate individual wheel rotation speed using traction control alone, especially when changes in vehicle configuration are large.

Here, we propose configuration-based wheel control that improves vehicle negotiation of irregular terrain by reducing wheel slippage and rotation error based on two key concepts. The first involves deriving movement speed

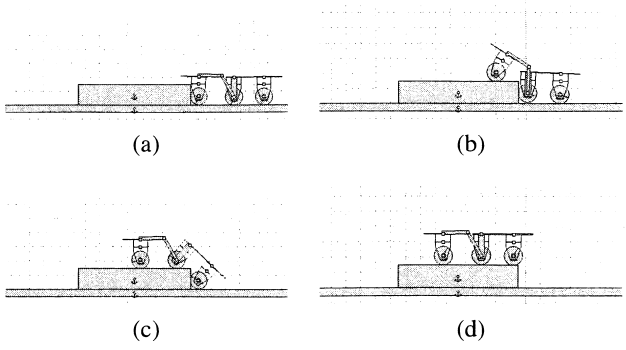

Fig. 3. Step climbing.

for individual wheels based on the vehicle configuration during step climbing in real time.

The second involves wheel control referencing while maintaining the balance of rotation speed among wheels, especially during step climbing with considering loads among wheels. Based on these two concepts, our vehicle uses suitable wheel control references referring to vehicle configuration while balancing wheel rotation speeds.

This paper is organized as follows: Section 2 discusses new control derivation referencing the vehicle configuration. Section 3 details results of experiments using our prototype. Section 4 presents conclusions.

2. Control

2.1. Kinematics

Our vehicle's built-in the passive links enable it to change configuration based on the terrain as it negotiates steps (**Fig. 3**), modifying wheel control by referencing its configuration. Here, we consider the relationship between wheel rotation velocity vectors and changes in vehicle configuration in general passive-link vehicle models.

We assume that the vehicle has n passive links and all wheels touch the ground and are activated. When the vehicle negotiates a barrier (**Fig. 4(a)**), the velocity vector of wheel $i+1$ is calculated by the velocity vector of wheel i and the rotation velocity vector of wheel $i+1$ in Eq. (1), expressed three-dimensionally Cartesian coordinations:

$$ {}^{i}\mathbf{v}_{i+1} = {}^{i}\mathbf{v}_{i} + {}^{i}\boldsymbol{\sigma}_{i} \times {}^{i}\mathbf{P}^{i}_{i+1} \quad \ldots\ldots\ldots\ldots (1) $$

where i is the number of wheel ($i = 1,\ldots,n$), ${}^{i}\mathbf{v}_{i}$ and ${}^{i}\boldsymbol{\sigma}_{i}$ are the velocity vector and the rotation vector of wheel i in Cartesian coordinate $\{i\}$. ${}^{i}\mathbf{P}^{i}_{i+1}$ is the position vector from wheel i to wheel $i+1$ on coordinate $\{i\}$.

Coordinates of each wheel are defined as follows (**Fig. 4(b)**):

(1) x-axis defined in wheel drive direction.

(2) y-axis defined perpendicular to the ground.

The x-direction of the velocity vector of coordinate $\{i\}$ is derived as the control reference. The control reference

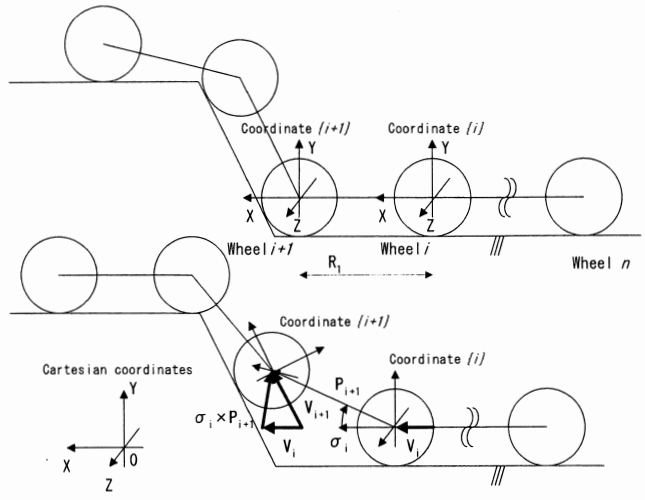

(a) Configuration

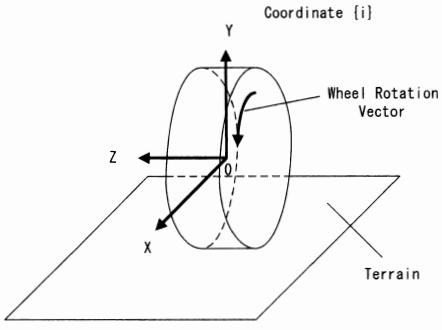

(b) Wheel model

Fig. 4. Relationship between velocity vector and vehicle.

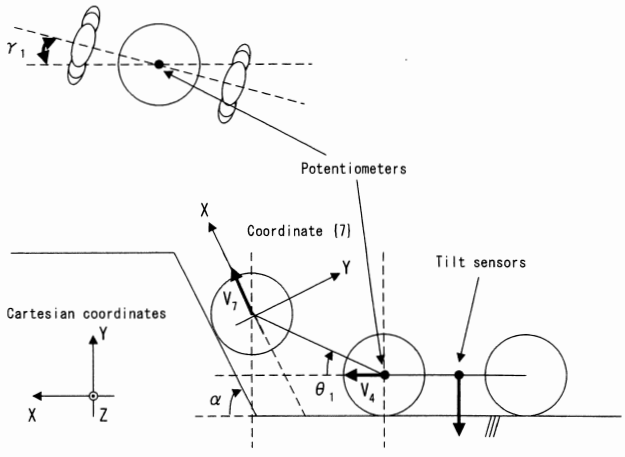

(a) Side

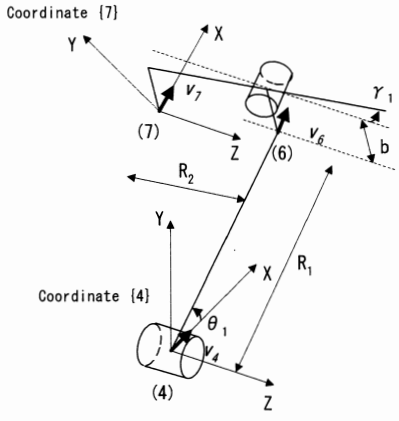

(b) 3D

Fig. 5. Prototype coordinates and parameters.

of wheel $i+1$ (ω_{i+1}) is derived from Eqs. (2) and (3):

$$\omega_{i+1} = \frac{\left\|{}^{i+1}\mathbf{v}_{i+1}\right\|_x}{r} + \left\|{}^{i}\boldsymbol{\sigma}_i\right\|_z \quad \ldots\ldots\ldots (2)$$

$${}^{i+1}\mathbf{v}_{i+1} = {}^{i+1}_{i}\mathbf{R} \cdot {}^{i}\mathbf{v}_{i+1}. \quad \ldots\ldots\ldots (3)$$

$\left\|{}^{i+1}\mathbf{v}_{i+1}\right\|_x$ is x-ingredient of the wheel $i+1$ velocity vector, r is the radius of the wheel and ${}^{i+1}_{i}\mathbf{R}$ is the conversion matrix from coordinate $\{i\}$ to $\{i+1\}$. When the velocity vector and rotation vector of wheel i are defined as ${}^{i}\mathbf{v}_i$ and ${}^{i}\boldsymbol{\sigma}_i$, the control reference of wheel $i+1$ is expressed as shown in Eq. (4):

$$\omega_{i+1} = \frac{\left\|{}^{i+1}_{i}\mathbf{R} \cdot \left({}^{i}\mathbf{v}_i + {}^{i}\boldsymbol{\sigma}_i \times {}^{i}\mathbf{P}^{i}_{i+1}\right)\right\|_x}{r} + \left\|{}^{i}\boldsymbol{\sigma}_i\right\|_z. \quad (4)$$

All wheels touch the ground, i.e., the plane shown in **Fig. 4(b)**. When the angle between the x-axis of coordinate $\{i\}$ and that of coordinate $\{i+1\}$ is α as shown in **Fig. 4(a)**, the conversion matrix is derived as shown in Eq. (5), and α fulfills Eq. (6):

$${}^{i+1}_{i}\mathbf{R} = \begin{bmatrix} \cos\alpha & -\sin\alpha & 0 \\ \sin\alpha & \cos\alpha & 0 \\ 0 & 0 & 1 \end{bmatrix} \quad \ldots\ldots (5)$$

$$\left\|{}^{i+1}\mathbf{v}_{i+1}\right\|_y = 0. \quad \ldots\ldots\ldots\ldots (6)$$

2.2. Prototype Adaptation

In the previous section, we discussed general vehicle kinematics referencing the vehicle configuration. Here, we adapt this to our vehicle prototype and derive the velocity vector of each wheel. Our vehicle measures changes in vehicle configuration using attitude sensors and generates wheel control references based on this information.

Our vehicle has two potentiometers on each passive joint and tilt sensors on the back (**Fig. 5(a)**). We measure the following angles using these sensors:

(1) Roll angle θ_1 and pitch angle γ_1 from potentiometers.

(2) Roll angle θ_2 and pitch angle γ_2 from tilt sensors.

Our vehicle has 7 actuated wheels. **Fig. 1(a)** defines the wheel number (wheel i: $i = 1, \ldots, 7$), coordinates, the length of individual links, and the rotate speed of each wheel. R_1 and R_2 indicate the length of each link and $\omega_1, \ldots, \omega_7$ are the rotation speeds of each wheel.

When the vehicle runs at v_0 in direction x on coordinate $\{4\}$, the velocity vector of wheel 7 on coordinate $\{4\}$ is derived as shown in Eq. (7) by Eq. (1). The kinematic

relationship among wheels is shown in **Fig. 5(b)**.

$$
\begin{aligned}
{}^4\mathbf{v}_7 &= {}^4\mathbf{v}_6 + {}^4\boldsymbol{\sigma}_6 \times {}^4\mathbf{P}_7^6 \\
&= ({}^4\mathbf{v}_4 + {}^4\boldsymbol{\sigma}_4 \times {}^4\mathbf{P}_6^4) + {}^4\boldsymbol{\sigma}_6 \times {}^4\mathbf{P}_7^6 = \begin{bmatrix} {}^4v_{7x} \\ {}^4v_{7y} \\ {}^4v_{7z} \end{bmatrix} \\
&= \begin{bmatrix} v_0 + \dot{\theta}_1\{-R_1\sin\theta_1 + R_2\cos\theta_1\sin\gamma_1 \\ \qquad -b\cos\theta_1(1-\cos\gamma_1)\} \\ \dot{\theta}_1\{R_1\cos\theta_1 - R_2\sin\theta_1\sin\gamma_1 + b\sin\theta_1 \\ \qquad \times(1-\cos\gamma_1)\} - \dot{\gamma}_1(R_2\cos\gamma_1 - b\sin\gamma_1) \\ -\dot{\gamma}_1(R_2\cos\theta_1\sin\gamma_1 - b\cos\theta_1(1-\cos\gamma_1)) \end{bmatrix} \\
&\qquad \cdots\cdots\cdots\cdots\cdots (7)
\end{aligned}
$$

Velocity vectors of wheels 1, 3, and 5 are derived from Eqs. (8), (9), and (10):

$$
\begin{aligned}
{}^4\mathbf{v}_1 &= \begin{bmatrix} {}^4v_{1x} & {}^4v_{1y} & {}^4v_{1z} \end{bmatrix}^T \\
&= \begin{bmatrix} v_0 - \dot{\theta}_2\{R_1\sin\theta_2 + R_2\cos\theta_2\sin\gamma_2 \\ \qquad -b\cos\theta_2(1-\cos\gamma_2)\} \\ \dot{\theta}_2\{R_1\cos\theta_2 + R_2\sin\theta_2\sin\gamma_2 - b\sin\theta_2 \\ \qquad \times(1-\cos\gamma_2)\} + \dot{\gamma}_2(R_2\cos\gamma_2 - b\sin\gamma_2) \\ \dot{\gamma}_2(R_2\cos\theta_2\sin\gamma_2 - b\cos\theta_2(1-\cos\gamma_2)) \end{bmatrix} \\
&\qquad \cdots\cdots\cdots\cdots\cdots (8)
\end{aligned}
$$

$$
\begin{aligned}
{}^4\mathbf{v}_3 &= \begin{bmatrix} {}^4v_{3x} & {}^4v_{3y} & {}^4v_{3z} \end{bmatrix}^T \\
&= \begin{bmatrix} v_0 + \dot{\theta}_2\{-R_1\sin\theta_2 + R_2\cos\theta_2\sin\gamma_2 \\ \qquad -b\cos\theta_2(1-\cos\gamma_2)\} \\ \dot{\theta}_2\{R_1\cos\theta_2 - R_2\sin\theta_2\sin\gamma_2 + b\sin\theta_2 \\ \qquad \times(1-\cos\gamma_2)\} - \dot{\gamma}_2(R_2\cos\gamma_2 - b\sin\gamma_2) \\ -\dot{\gamma}_2(R_2\cos\theta_2\sin\gamma_2 - b\cos\theta_2(1-\cos\gamma_2)) \end{bmatrix} \\
&\qquad \cdots\cdots\cdots\cdots\cdots (9)
\end{aligned}
$$

$$
\begin{aligned}
{}^4\mathbf{v}_5 &= \begin{bmatrix} {}^4v_{5x} & {}^4v_{5y} & {}^4v_{5z} \end{bmatrix}^T \\
&= \begin{bmatrix} v_0 - \dot{\theta}_1\{R_1\sin\theta_1 + R_2\cos\theta_1\sin\gamma_1 \\ \qquad -b\cos\theta_1(1-\cos\gamma_1)\} \\ \dot{\theta}_1\{R_1\cos\theta_1 + R_2\sin\theta_1\sin\gamma_1 - b\sin\theta_1 \\ \qquad \times(1-\cos\gamma_1)\} + \dot{\gamma}_1(R_2\cos\gamma_1 - b\sin\gamma_1) \\ \dot{\gamma}_1(R_2\cos\theta_1\sin\gamma_1 - b\cos\theta_1(1-\cos\gamma_1)) \end{bmatrix} \\
&\qquad \cdots\cdots\cdots\cdots\cdots (10)
\end{aligned}
$$

The rotation vector of each wheel is derived using roll and pitch angles as shown in Eqs. (11) and (12). In Eq. (11), the rotation vectors of wheels 5 and 7 are the same because these wheels are connected by the same link. Similarly, the rotation vectors of wheels 1 and 3 are the same in Eq. (12).

$$
\begin{aligned}
{}^4\boldsymbol{\sigma}_5 = {}^4\boldsymbol{\sigma}_7 &= \begin{bmatrix} {}^4\sigma_{7x} & {}^4\sigma_{7y} & {}^4\sigma_{7z} \end{bmatrix}^T \\
&= \begin{bmatrix} \dot{\gamma}_1 & 0 & \dot{\theta}_1 \end{bmatrix}^T \cdots\cdots (11)
\end{aligned}
$$

$$
\begin{aligned}
{}^4\boldsymbol{\sigma}_1 = {}^4\boldsymbol{\sigma}_3 &= \begin{bmatrix} {}^4\sigma_{3x} & {}^4\sigma_{3y} & {}^4\sigma_{3z} \end{bmatrix}^T \\
&= \begin{bmatrix} \dot{\gamma}_2 & 0 & \dot{\theta}_2 \end{bmatrix}^T \cdots\cdots (12)
\end{aligned}
$$

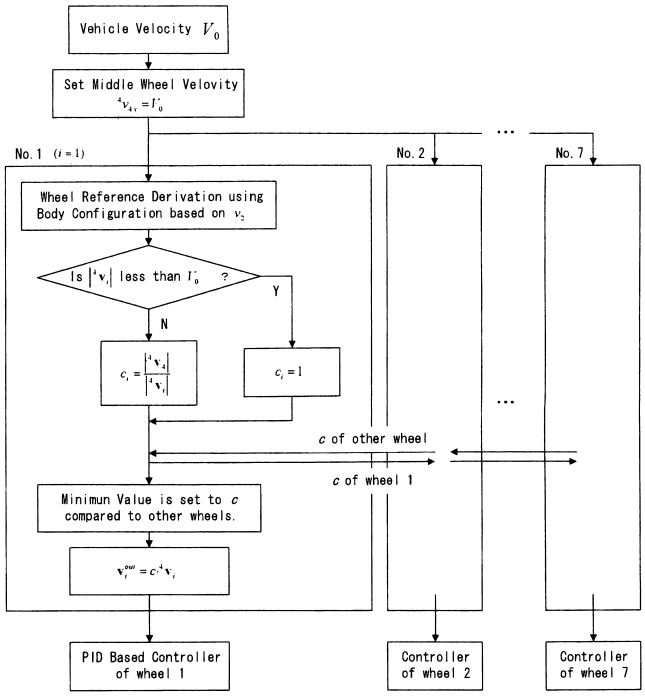

Fig. 6. Wheel control reference flowchart.

2.3. Wheel Control Reference Derivation

Having derived velocity vectors and individual wheel rotation vectors when the vehicle runs at v_0 on coordinate $\{4\}$, these vectors are calculated using only the kinematic relationship of the wheels. Velocity vectors vary greatly when the vehicle configuration changes greatly. Simply deriving wheel control references using these extraordinary vectors in Eq. (4), yields equally varying that prevent the vehicle from balancing wheel rotation speeds and causing wheel slippage and rotation error. To derive suitable wheel control references from results in the previous section, we consider the following:

(1) When the vehicle negotiates the step at V_0 along the vehicle coordinate (**Fig. 1(a)**), we set V_0 as the velocity in direction x on the coordinate $\{4\}$.

(2) To maintain balance among wheel rotation speeds, all wheel speed based on V_0 referencing the vehicle configuration must be smaller than V_0 (**Fig. 6**).

When the vehicle negotiates the step at V_0 on the vehicle coordinate (**Fig. 1(a)**), we set the speed in direction x on coordinate $\{4\}$ as shown in Eq. (13) temporarily and we derive velocity vectors of all wheels from Eqs. (7)-(10):

$$
{}^4v_{4x} = V_0 \cdots\cdots\cdots\cdots\cdots (13)
$$

Coefficient c_i of wheel i is determined by Eq. (14):

$$
c_i = \begin{cases} \dfrac{|V_0|}{|{}^4\mathbf{v}_i|} & \text{if} \quad |{}^4\mathbf{v}_i| > |V_0| \\ 1 & \text{if} \quad |{}^4\mathbf{v}_i| \le |V_0| \end{cases} \cdots\cdots (14)
$$

where ${}^4\mathbf{v}_i$ indicates the calculated velocity vector of wheel i. i $(=1,\ldots,7)$ indicates subnumber for identifying wheels.

The velocity vector on coordinate $\{4\}$ is determined as shown in Eq. (15), in which all wheel velocity vectors are calculated within the range of V_0:

$$\mathbf{v}_i^{out} = c \cdot {}^4\mathbf{v}_i \quad \ldots\ldots\ldots\ldots\ldots\ldots (15)$$

where $c = \min\{c_1,\ldots,c_7\}$.

We derive wheel control references from wheel velocity and rotation vectors derived in the previous section. When we set v_0 as velocity vector $\mathbf{v}_4^{out}$ of direction x, the velocity vector of wheel i on coordinate $\{i\}$ is as shown in Eq. (16). As shown in Eq. (5), we assume that the obstacle is a α-degree slope for each wheel (**Fig. 5(a)**).

$$ {}^i\mathbf{v}_i = {}^i_4\mathbf{R} \cdot {}^4\mathbf{v}_i = \begin{bmatrix} \cos\alpha & -\sin\alpha & 0 \\ \sin\alpha & \cos\alpha & 0 \\ 0 & 0 & 1 \end{bmatrix} \cdot \begin{bmatrix} {}^4v_{ix} \\ {}^4v_{iy} \\ {}^4v_{iz} \end{bmatrix} $$
$$ = \begin{bmatrix} \cos\alpha \cdot {}^4v_{ix} - \sin\alpha \cdot {}^4v_{iy} \\ \sin\alpha \cdot {}^4v_{ix} + \cos\alpha \cdot {}^4v_{iy} \\ {}^4v_{iz} \end{bmatrix} \quad \ldots\ldots (16)$$

From Eqs. (4) and (13), the control reference of wheel i is expressed as shown in Eq. (17):

$$\omega_i = \frac{\cos\alpha \cdot {}^4v_{ix} - \sin\alpha \cdot {}^4v_{iy}}{r} + {}^4\sigma_{iz}. \quad \ldots\ldots (17)$$

The α degree is defined as shown in Eq. (18) because the x axis is defined in the wheel drive direction and the velocity vector is parallel to the drive direction as shown in Eq. (6):

$$\sin\alpha \cdot {}^4v_{ix} + \cos\alpha \cdot {}^4v_{iy} = 0. \quad \ldots\ldots\ldots (18)$$

Our vehicle controls each wheel based on this control reference using PID-based control that coordinates the output traction of each wheel [17].

3. Experiments

3.1. Setup

We verify the effectiveness of our proposed control reference in experiments using our prototype (**Fig. 7**). Our prototype negotiates the step while moving forward.

Adapting our proposed control reference to our prototype, we compare the result of the proposed reference to the result of a fixed reference without considering the vehicle configuration. Vehicle parameters are given in **Table 1**.

We conducted two experiments. In the first, the vehicle negotiates the same step twice – once using our proposed control and once without using it. The vertical gap in the step is 0.065 m and we evaluate wheel slippage and rotation error. In the second, we verify the maximum step height that the vehicle can negotiate.

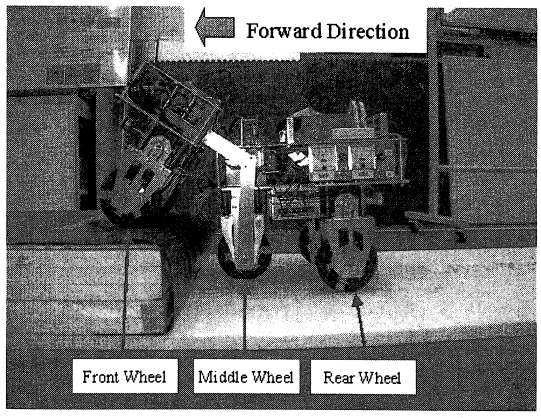

Fig. 7. Setup.

Table 1. Prototype parameters.

Linkage Number	2
Linkage Length	Front 195 mm, Back 400 mm
Weight	Front 7.8 kg, Back 13.8 kg
Wheel Diameter	132 mm
Distance between Wheels	Front-Middle 255 mm, Middle-Rear 215 mm
Friction Coefficient	Static 0.3, Dynamic 0.25
Speed (V_0)	0.25 m/s

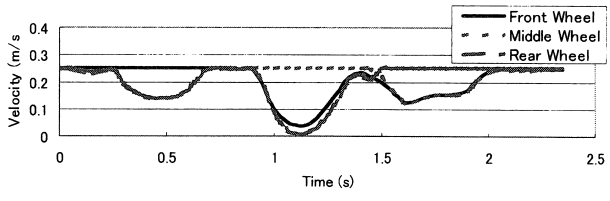

Fig. 8. Wheel control reference during climbing.

3.2. Results (1)

When the vehicle prototype negotiates the 0.065 m step in experiment 1, control references for each wheel are derived as shown in **Fig. 8**. These references are within the range of V_0 and the experiment verifies that these control references are suitable.

Figure 9 shows the slippage ratio [16] and **Fig. 10** the rotation error ratio of wheels during climbing. Three peaks show contact between the step and the front, middle, and rear wheel. The wheel slippage ratio decreases to 45% and the wheel rotation error ratio decreases to 43% under our proposed control scheme (**Table 2**). The wheel slippage ratio and rotation error ratio are calculated using Eqs. (19) and (20):

$$\hat{s} = \frac{r\omega - v_\omega}{r\omega} \quad \ldots\ldots\ldots\ldots\ldots (19)$$

$$\hat{d} = \frac{\omega_{ref} - \omega}{\omega} \quad \ldots\ldots\ldots\ldots\ldots (20)$$

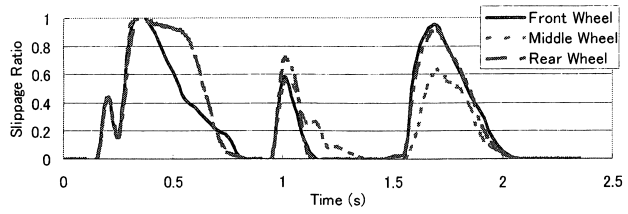

(a) Fixed control reference

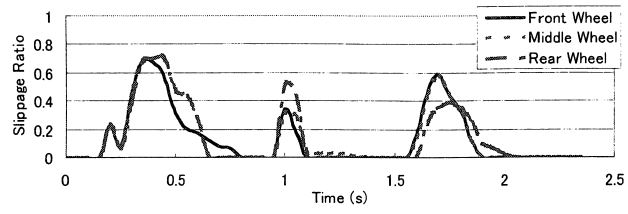

(b) Proposed control reference

Fig. 9. Wheel slippage ratio.

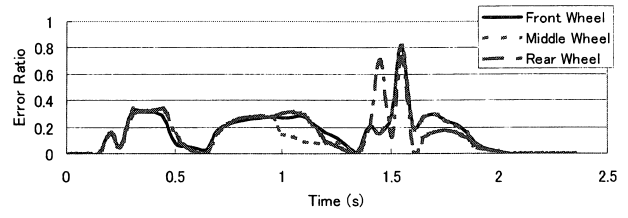

(a) Fixed control reference

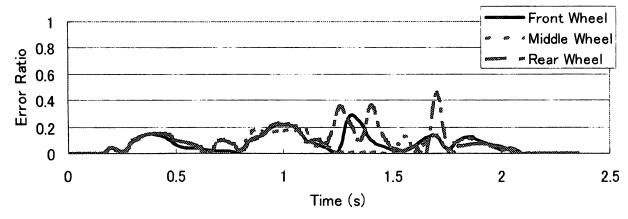

(b) Proposed control reference

Fig. 10. Wheel rotation error ratio.

Table 2. Wheel slippage and rotation error ratio [%].

Ratio \ Wheel	Reference	Front	Middle	Rear	Average
Slippage	Fixed	26.7	25.9	24.4	25.7
	Proposed	12.9	12.0	10.4	11.7
Rotation Error	Fixed	32.5	29.8	30.7	31.0
	Proposed	12.7	13.4	14.2	13.4

where ω is the wheel rotation speed and ω_{ref} the wheel rotation speed reference. r and v_ω indicate the radius of the wheel and the vehicle speed.

These results confirm that our proposed scheme reduces wheel slippage and rotation error.

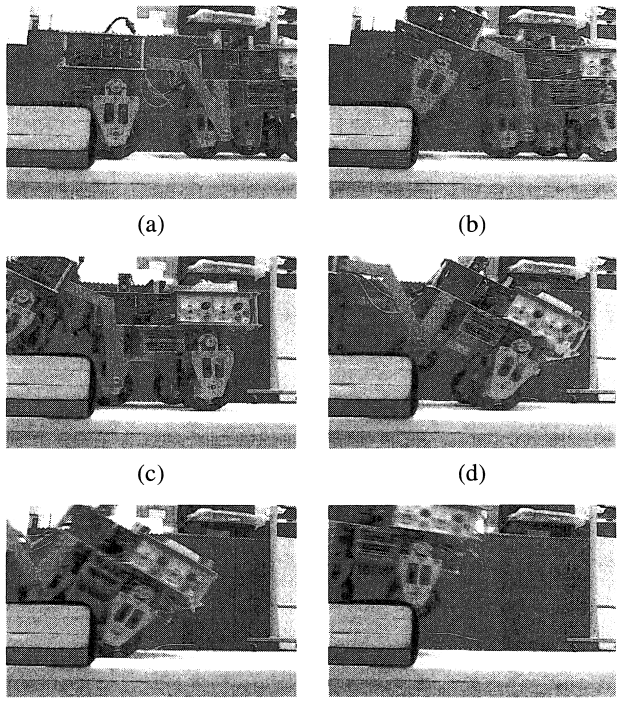

(a) (b) (c) (d) (e) (f)

Fig. 11. Negotiating a 152 mm step using wheels 132 mm in diameter.

3.3. Results (2)

In experiment 2, the vehicle negotiated a 0.152 m step based on our proposed wheel control scheme (**Fig. 11**). With the standard scheme, the vehicle can negotiate only a 0.072 m step. Our vehicle can negotiate 0.180 m based on mechanical design, so our control realizes 85% of the vehicle's potential step-climbing performance. Experimental results verify that vehicle performance increases using our proposed wheel control.

4. Conclusions

We have proposed step-climbing wheel control based on vehicle configuration changes during climbing. We discuss a configuration-based kinematic model for which we adjust wheel control, enabling the vehicle to maintain its balance through rotation speeds while negotiating steps.

Results of experiments verified the effectiveness of our proposed. Based on our approach, the wheel slippage ratio and rotation error ratio decreased when our vehicle negotiated the steps, improving its performance. Our vehicle negotiated 0.152 m steps using wheels 0.132 m in diameter. Our omnidirectional wheel control scheme is useful for wheeled vehicles with passive links.

References:

[1] G. Campion, G. Bastin, and B. D. Andrea-Novel, "Structural Properties and Classification of Kinematic and Dynamic Models of Wheeled Mobile Robots," in IEEE Trans. on Robotics and Automation, Vol.12, No.1, pp. 47-62, 1996.

[2] M. Ichikawa, "Wheel arrangements for Wheeled Vehicle," Journal of the Robotics Society of Japan, Vol.13, No.1, pp. 107-112, 1995.

[3] G. Endo and S. Hirose, "Study on Roller-Walker: System Integration and Basic Experiments," in Proc. of the 1999 IEEE Int. Conf. on Robotics & Automation, pp. 2032-2037, 1999.

[4] T. McGeer, "Passive dynamic walking," The Int. Journal of Robotics Research, Vol.9, No.2, pp. 62-82, 1990.

[5] M. Wada and H. Asada, "Design and Control of a Variable Footpoint Mechanism for Holonomic Omnidirectional Vehicles and its Application to Wheelchairs," in IEEE Trans. on Robotics and Automation, Vol.15, No.6, pp. 978-989, 1999.

[6] S. Hirose and S. Amano, "The VUTON: High Payload, High Efficiency Holonomic Omni-Directional Vehicle," in Proc. of the 6th Symp. on Robotics Research, pp. 253-260, 1993.

[7] D. Chugo, K. Kawabata, H. Kaetsu, H. Asama, and T. Mishima, "Development of omni-directional vehicle with step-climbing ability," in Proc. of the 2003 IEEE Int. Conf. on Robotics and Automation, pp. 3849-3854, 2003.

[8] H. Asama, M. Sato, L. Bogoni, H. Kaetsu, A. Matsumoto, and I. Endo, "Development of an Omni-Directional Mobile Robot with 3 DOF Decoupling Drive Mechanism," in Proc. of the 1995 IEEE Int. Conf. on Robotics and Automation, pp. 1925-1930, 1995.

[9] H. W. Stone, "Mars Pathfinder Microrover: A Low-Cost, Low-Power Spacecraft," in Proc. of the 1996 AIAA Forum on Advanced Developments in Space Robotics, 1996.

[10] M. Thianwiboon, V. Sangveraphunsiri, and R. Chancharoen, "Rocker-Bogie Suspension Performance," The 11th Int. Pacific Conf. in Automotive Engineering, Shanghai, China, IPC2001D079, 2001.

[11] D. Chugo, K. Kawabata, H. Kaetsu, H. Asama, and T. Mishima, "Mechanical Design of Step-Climbing Vehicle with Passive Linkages," in Proc. of the 8th Int. Conf. on Climbing and Walking Robots, pp. 287-294, 2005.

[12] B. Carisle, "An Omni-Directional Mobile Robot," Developments in Robotics 1983, IFS Publications Ltd., pp. 79-87, 1983.

[13] D. Chugo, K. Kawabata, H. Kaetsu, H. Asama, and T. Mishima, "Development of Control System for Omni directional Vehicle with Step-Climbing Ability," in Proc. of the 4th Int. Conf. on Field and Service Robotics, pp. 121-126, 2003.

[14] Y. Kuroda, K. Kondo, K. Nakamura, Y. Kunii, and T. Kubota, "Low Power Mobility System for Micro Planetary Rover Micro5," in Proc. of the 5th Int. Symp. on Artificial Intelligence, Robotics and Automation in Space (i-SAIRAS99), pp. 77-82, 1999.

[15] P. Lamon, A. Krebs, M. Lauria, S. Shooter, and R. Siegwart, "Wheel torque control for a rough terrain rover," in Proc. of the Int. Conf. on Robotics and Automation, pp. 4682-4687, 2004.

[16] K. Yoshida and H. Hamano, "Motion Dynamic of a Rover With Slip-Based Traction Model," in Proc. of the 2002 IEEE Int. Conf. on Robotics & Automation, pp. 3155-3160, 2001.

[17] D. Chugo, K. Kawabata, H. Kaetsu, H. Asama, and T. Mishima, "Development of a Control System for an Omni directional Vehicle with Step-Climbing Ability," Advanced Robotics, Vol.19, No.1, pp. 51-71, 2005.

Name:
Daisuke Chugo

Affiliation:
Research Associate, Graduate School of Information Systems, The University of Electro-Communications

Address:
1-5-1 Chofugaoka, Chofu, Tokyo 182-8585, Japan

Brief Biographical History:
2005- Postdoctral Researcher of Intelligent Modeling Lab. (IML), The University of Tokyo
2005- Postdoctral Researcher of Research into Artifacts, Center for Engineering (RACE), The University of Tokyo
2006- Research Associate of Graduate School of Information Systems, The University of Electro-Communications

Main Works:
- "Development of a Control System for an Omni directional Vehicle with Step-Climbing Ability," Advanced Robotics, Vol.19, No.1, pp. 51-71, 2005.

Membership in Academic Societies:
- Institute of Electrical and Electronics Engineers, Inc. (IEEE)
- The Japan Society of Mechanical Engineers (JSME)
- The Robotics Society of Japan (RSJ)
- Japan Society for Design Engineering (JSDE)

Name:
Kuniaki Kawabata

Affiliation:
Unit Leader, Distributed Adaptive Robotics Research Unit, RIKEN (The Institute of Physical and Chemical Research)

Address:
2-1 Hirosawa, Wako, Saitama 351-0198, Japan

Brief Biographical History:
1997- Special postdoctral researcher, Biochemical Systems Lab. at RIKEN
2000- Research scientist, Advanced Engineering Center at RIKEN
2002- Distributed Adaptive Robotics Research Unit, RIKEN
2005- Unit Leader of Distributed Adaptive Robotics Research Unit, RIKEN

Main Works:
- Distributed Autonomous Robotic Systems, Intelligent Ubiquitous Information Device Machine Learning and Visual Perception

Membership in Academic Societies:
- The Japan Society of Mechanical Engineering (JSME)
- The Robotics Society of Japan (RSJ)
- The Japanese Society of Instrumentation and Control Engineers (SICE)
- The Institute of Electrical Engineers of Japan (IEEJ)
- The Japanese Society for Artificial Intelligence (JSAI)
- The Institute of Electrical and Electronics Engineers, Inc. (IEEE)

Name:
Hayato Kaetsu

Affiliation:
Senior Engineer, Distributed Adaptive Robotics Research Unit (DARS), RIKEN (The Institute of Physical and Chemical Research)

Address:
2-1 Hirosawa, Wako, Saitama 351-0198, Japan

Brief Biographical History:
1971- Radioisotope Technology Division, RIKEN
1986- Biochemical Systems Lab., RIKEN
2002- Distributed Adaptive Robotics Research Unit, RIKEN

Main Works:
• Separation of radioisotope object, Distributed autonomous robotic systems (DARS)

Membership in Academic Societies:
• The Japan Society of Mechanical Engineering (JSME)
• Japan Society for Precision Engineering (JSPE)

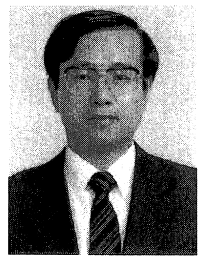

Name:
Taketoshi Mishima

Affiliation:
Professor, Saitama University

Address:
255 Shimo-Ookubo, Sakura-ku, Saitama, Saitama 338-8570, Japan

Brief Biographical History:
1974- Research Scientist, ETL, AIST, Ministry of International Trade and Industry (MITI)
1992- Professor, Josai International University
1993- Professor, Saitama University

Main Works:
• "Scale Invariant Face Detection and Classification Method using Shift Invariant Features Extracted from Log-Polar Image," Transactions of The Institute of the Electronics, Information and Communication Engineers (IEICE), Information and Systems, Vol.JE84-D, No.7, pp. 867-878, 2001.

Membership in Academic Societies:
• The Institute of Electronics, Information and Communication Engineers (IEICE)
• Mathematical Society of Japan (MSJ)

Name:
Hajime Asama

Affiliation:
Professor, Research into Artifacts, Center for Engineering (RACE), The University of Tokyo

Address:
5-1-5 Kashiwanoha, Kashiwa, Chiba 277-8568, Japan

Brief Biographical History:
1986- Research Associate of RIKEN (The Institute of Physical and Chemical Research)
1998- Senior Scientist of RIKEN (The Institute of Physical and Chemical Research)
2002- Professor of Research into Artifacts, Center for Engineering (RACE), The University of Tokyo

Main Works:
• "Distributed Task Processing by a multiple Autonomous Robot System Using an Intelligent Data Carrier System," Intelligent Automation and Soft Computing, An International Journal, Vol.6, No.3, pp. 215-224, 2000.

Membership in Academic Societies:
• Institute of Electrical and Electronics Engineers, Inc. (IEEE)
• The Japan Society of Mechanical Engineers (JSME)
• The Robotics Society of Japan (RSJ)
• The Japanese Society of Instrumentation and Control Engineers (SICE)